

A3E: Aligned and Augmented Adversarial Ensemble for Accurate, Robust and Privacy-Preserving EEG Decoding

Xiaoqing Chen, Tianwang Jia, Dongrui Wu

Abstract—An electroencephalogram (EEG) based brain-computer interface (BCI) enables direct communication between the brain and external devices. However, EEG-based BCIs face at least three major challenges in real-world applications: data scarcity and individual differences, adversarial vulnerability, and data privacy. While previous studies have addressed one or two of these issues, simultaneous accommodation of all three challenges remains challenging and unexplored. This paper fills this gap, by proposing an Aligned and Augmented Adversarial Ensemble (A3E) algorithm and integrating it into three privacy protection scenarios (centralized source-free transfer, federated source-free transfer, and source data perturbation), achieving simultaneously accurate decoding, adversarial robustness, and privacy protection of EEG-based BCIs. Experiments on three public EEG datasets demonstrated that our proposed approach outperformed over 10 classic and state-of-the-art approaches in both accuracy and robustness in all three privacy-preserving scenarios, even outperforming state-of-the-art transfer learning approaches that do not consider privacy protection at all. This is the first time that three major challenges in EEG-based BCIs can be addressed simultaneously, significantly improving the practicalness of EEG decoding in real-world BCIs.

Index Terms—Electroencephalogram, brain-computer interface, privacy protection, adversarial robustness, transfer learning

I. INTRODUCTION

A brain-computer interface (BCI) creates a direct link between the human brain and a computer, allowing the assistance, improvement, or recovery of cognitive and/or sensory-motor functions [1]. BCIs have broad applications in neurological rehabilitation [2], touch-based exploration [3], robot control [4], speech synthesis [5], and so on.

BCIs can be grouped into non-invasive, partially invasive, and invasive ones. Among these, non-invasive BCIs, which often use electroencephalogram (EEG) signals [6], are the most popular due to their ease of use. Motor imagery (MI) is a classic paradigm of EEG-based BCIs [7], in which the user imagines the movement of specific body parts (e.g., left hand, right hand, both feet, or tongue) to activate different brain parts. These imagined movements are decoded from EEG and converted into commands for external devices.

A typical closed-loop EEG-based BCI system includes four essential parts: signal acquisition, signal processing, machine learning, and a controller, as shown in Figure 1.

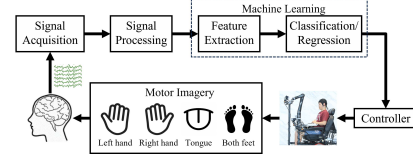


Fig. 1: Flowchart of a closed-loop EEG-based BCI system.

Despite various advantages like non-invasiveness and low cost, real-world EEG-based BCIs face at least three challenges:

- 1) *Data scarcity and individual differences.* Collecting EEG signals is time-consuming and labor-intensive, and hence the amount of training data is usually small. Additionally, EEG responses vary widely across users, making it challenging, if not impossible, to apply a decoding model trained on one subject to another. Data scarcity and individual differences significantly reduce EEG decoding accuracy [8].
- 2) *Adversarial vulnerability.* BCI outputs can be easily manipulated by adversarial attacks [9]–[15]. Zhang and Wu [9] first discovered that adversarial samples significantly reduce the decoding accuracy of EEG-based BCIs. Liu *et al.* [11] and Jung *et al.* [14] later developed universal adversarial perturbations, making such attacks easier to implement. Wang *et al.* [12] explored physically constrained attacks. Bian *et al.* [13] used square wave signals to attack steady-state visual evoked potential based BCIs. Gunawardena *et al.* [16] further tested sparse perturbation attacks in grey-box and black-box settings. Meng *et al.* [17] investigated adversarial attacks to regression tasks in BCIs. These attacks expose serious safety concerns of BCIs, making adversarial robustness a critical consideration.
- 3) *User privacy.* Recently, multiple laws and regularization on user privacy protection has been established, e.g., the European Union General Data Protection Regulation, and the China Personal Information Protection Law. EEG data contain sensitive private information, regardless of the paradigm involved [18], [19]. For example, Martinovic *et al.* [20] showed that private information like credit card numbers, personal identification numbers, known contacts, and addresses, may be inferred from EEG signals. Ikena *et al.* [1] highlighted ethical concerns and privacy issues with consumer neurotechnology. Landau *et al.* [21] found that even resting-state

EEG data can reveal personality traits and cognitive abilities.

Extensive research has been conducted to address these three challenges individually. For example, transfer learning improves the BCI classification accuracy by using EEG data from other subjects [8], [22]; adversarial detection and robust training enhance the robustness of BCIs [23], [24]; and, privacy-preserving machine learning and data perturbation help protect the privacy of EEG data [25], [26]. However, accommodating one challenge may sometimes degrade the model performance in other aspects. For example, cross-user transfer learning may expose the privacy of source users, while adversarial defense may reduce the classification accuracy on benign samples [23].

Some recent studies have also attempted to address two of these three challenges simultaneously. For instance, alignment-based adversarial training (ABAT) [27] improves both the accuracy and adversarial robustness of the classifier, and privacy-preserving transfer learning [25], [28] enhances model classification accuracy while safeguarding the source data privacy.

However, to our knowledge, no study so far can address all three challenges simultaneously. This paper fills this gap. We demonstrate for the first time that it is feasible to achieve simultaneously accuracy, robust and privacy-preserving decoding of EEG-based BCIs through a single classifier. More specifically, we first propose aligned and augmented adversarial ensemble (A3E), which leverages data alignment, data augmentation, adversarial training, and ensemble learning to improve the classification accuracy and robustness, and then integrate it into three privacy-preserving transfer learning scenarios:

- 1) Centralized source-free transfer learning, where only a source model (instead of source data) is shared to facilitate the classification for the target user. If there are multiple source domains, their data can be pooled together to train a single source model.
- 2) Federated source-free transfer learning, which considers a more strict privacy protection scenario that EEG data from different source users cannot be combined for joint training.
- 3) Source data perturbation, where the source domain EEG data are perturbed to make user-specific private information unlearnable while preserving the task-relevant information. The perturbed source EEG data can then be used to assist the training of the target model, without compromising the privacy of the source users.

Experiments on three public EEG datasets demonstrated that our approach outperformed over 10 classical and state-of-the-art approaches in accuracy and robustness across all three privacy protection scenarios, including those transfer learning algorithms that do not consider privacy protection at all.

In summary, our main contributions are:

- 1) We propose A3E, which leverages data alignment, data augmentation, adversarial training, and ensemble learning to improve simultaneously the classification accuracy and adversarial robustness.

- 2) We integrate A3E with privacy-preserving transfer learning, achieving for the first time simultaneous accurate decoding, adversarial robustness, and privacy protection.
- 3) We consider three diverse privacy-protection scenarios, i.e., centralized source-free transfer learning, federated source-free transfer learning, and source data perturbation, demonstrating the generalization and flexibility of our approach.

The remainder of this paper is organized as follows: Section II describes related works. Section III introduces our proposed approach. Section IV describes the experimental settings. Section V presents the experimental results. Finally, Section VI draws conclusions.

II. RELATED WORK

This section introduces related works on transfer learning, adversarial defense, and privacy protection.

A. Transfer Learning

Transfer learning uses data from the source domains to facilitate the learning in the target domain. The challenge is to reduce the data distribution discrepancy between the source and target domains, represented by the marginal or conditional probability distributions, or their combination.

Marginal distribution discrepancy reduction strategies including input transformations, e.g., Euclidean Alignment (EA) [22], distribution alignments, e.g., Deep Adaptation Network (DAN) [29], and adversarial training, e.g., Domain-Adversarial Neural Network (DANN) [30]. Conditional distribution discrepancy reduction strategies include pseudo-labeling, e.g., Joint Adaptation Networks (JAN) [31], and uncertainty reduction, e.g., Minimum Class Confusion (MCC) [32] and Source Hypothesis Transfer (SHOT) [25]. Margin Disparity Discrepancy (MDD) [33] and Conditional Domain Adversarial Networks (CDAN) [34] are two representative joint marginal and conditional distribution discrepancy reduction approaches.

B. Adversarial Defense

Various adversarial defense approaches have been proposed in computer vision and natural language processing [35]. Among these, robust training [36], which adds adversarial samples to the training data, is one of the most effective strategies. Adversarial Training [35] is a well-known robust training approach, with many variants [37], [38].

Adversarial defense in BCIs has also received increasing attention [23], [27], [39], [40]. Li *et al.* [41] evaluated five adversarial training based defense approaches in BCIs. Meng *et al.* [23] provided a comprehensive assessment of the pros and cons of various adversarial defense strategies in BCIs. Gunawardena *et al.* [16] combined adversarial training with adversarial detection to defend against black-box attacks in EEG-based BCIs. However, previous studies show that while adversarial defenses can enhance the robustness, they often reduce the classification performance on benign samples [23], [41]. To address this issue, Chen *et al.* [27] proposed ABAT

for EEG-based BCIs, which performs adversarial training on aligned EEG data, improving the classification accuracy on benign and adversarial samples simultaneously.

C. Privacy Protection

Various privacy protection approaches have been proposed for EEG-based BCIs to prevent the leakage of private information in EEG data. They can be broadly categorized into two main types [19]:

- 1) *Privacy-preserving machine learning*, which avoids using raw EEG data or model parameters directly. Typical approaches include source-free transfer learning [28], [42], [43] and federated learning [44]. Data privacy is protected since the training data are not transferred. For example, Zhang *et al.* [42] studied gray-box and black-box transfer for MI and affective BCIs, and Jia *et al.* [44] restricted data transfer from clients to the server using federated learning.
- 2) *Data perturbation*, which adds perturbations to the original data to prevent machine learning models from learning private information while maintaining data utility for downstream tasks. For example, Meng *et al.* [45] designed sample-specific and user-specific perturbations to generate identity-unlearnable EEG data, and Chen *et al.* [26] further proposed four types of robust user-wise perturbations to protect privacy information in EEG.

III. ACCURATE, ROBUST, AND PRIVACY-PRESERVING EEG DECODING

This section introduces our proposed approach for accurate, robust, and privacy-preserving EEG-Based BCIs, including the A3E algorithm and three privacy-preserving scenarios.

A. Problem Statement

Consider a source EEG training dataset $\mathcal{D}_S = \{(X_{S,i}, y_{S,i}, u_i)\}_{i=1}^{N_S}$ consisting of N_S samples, where $X_{S,i} \in \mathbb{R}^{c \times t}$ is the i -th EEG trial with c channels and t time-domain samples, $y_{S,i} \in \{1, \dots, K\}$ is the corresponding BCI task label (e.g., left/right hand MI), and $u_i \in \{1, \dots, U\}$ denotes the user identity label. Additionally, we have a calibration dataset $\mathcal{D}_T = \{(X_{T,i}, y_{T,i})\}_{i=1}^{N_T}$ with N_T samples, where each $X_{T,i} \in \mathbb{R}^{c \times t}$ is an EEG trial with c channels and t time-domain samples, and $y_{T,i} \in \{1, \dots, K\}$ is the corresponding BCI task label.

\mathcal{D}_S contains both task-relevant and private information of the source users [26], so its direct access is restricted to safeguard user privacy. Instead, we only have access to a task model C_θ trained on \mathcal{D}_S , or a perturbed dataset $\tilde{\mathcal{D}}_S$ that masks user-specific information of \mathcal{D}_S in training the target domain classifier.

B. Overall Framework

In privacy-protection scenarios, the task model C_θ trained in the source domain or perturbed privacy-preserving source data $\tilde{\mathcal{D}}_S$ can be used to facilitate the training in the target domain using our proposed A3E, as shown in Figure 2 and Algorithm 1.

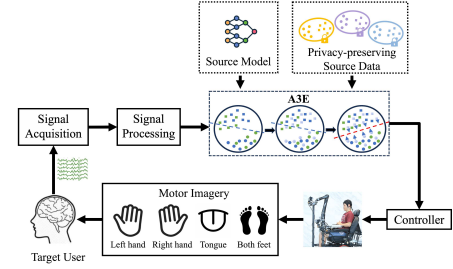


Fig. 2: Flowchart of a closed-loop EEG-based BCI system using source model or data.

Algorithm 1: Algorithm for accurate, robust and privacy-preserving EEG decoding.

Input: C_θ , task classifier trained in the source domain;
 $\tilde{\mathcal{D}}_S$, perturbed privacy-preserving source data;
 \mathcal{D}_T , target domain calibration EEG data;

Output: C'_θ , target classifier.

Perform data alignment on \mathcal{D}_T by (1) and (2);

Perform data augmentation on \mathcal{D}_T by (3) to obtain augmented calibration set \mathcal{D}'_T ;

// Centralized source-free transfer learning scenario, or federated source-free transfer learning scenario

Fine-tune C_θ on \mathcal{D}'_T by (4), (5) and (6) to obtain target classifier C'_θ ;

// Source data perturbation scenario

Train target classifier C'_θ on \mathcal{D}'_T and $\tilde{\mathcal{D}}_S$ by (5), (6) and (7).

C. Privacy Protection Scenarios

1) *Centralized Source-Free Transfer Learning*: In this scenario, the source users trust each other, so they can share raw EEG data among themselves, but not with the target user. EEG data from multiple source users are aggregated to train a single source model, which is then utilized in transfer learning to train the target model, as illustrated in Figure 3. As the target user cannot access the source domain data, the source data privacy is protected.

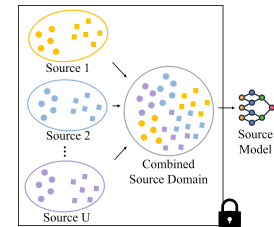


Fig. 3: Illustration of the centralized source-free transfer learning scenario.

2) *Federated Source-Free Transfer Learning*: In this more strict privacy-protection scenario, no source user wants to share his/her raw EEG data with other source users and the target user. A central server, without access to the source users'

private EEG data, maintains a global model and distributes it to each source user for updates. Each source user refines the global model parameters using his/her own EEG data and sends these updates back to the server for aggregation, as illustrated in Figure 4. Our recently proposed federated learning algorithm [44], which achieves superior performance compared to centralized training, is utilized in this paper.

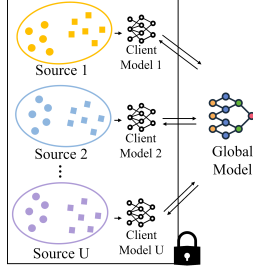


Fig. 4: Illustration of the federated source-free transfer learning scenario.

3) *Source Data Perturbation*: A user-specific perturbation can be applied to each source domain to safeguard source user privacy while still leveraging the source data for target domain classifier training, as illustrated in Figure 5. This perturbation makes the user identity information unlearnable while preserving the BCI task related information. Our recently proposed privacy-preserving perturbation approach [26] is utilized in this paper.

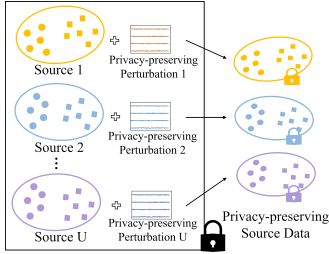


Fig. 5: Illustration of the source data perturbation scenario.

Given a source EEG training dataset $\mathcal{D}_S = \{(X_{S,i}, y_{S,i}, u_i)\}_{i=1}^{N_S}$, we generate a privacy-unlearnable EEG training dataset $\tilde{\mathcal{D}}_S = \{(\tilde{X}_{S,i}, y_{S,i}, u_i)\}_{i=1}^{N_S}$, by adding a user-wise perturbation $\Delta_{u_i} \in \mathbb{R}^{c \times t}$ to each EEG trial $X_{S,i}$, i.e., $\tilde{X}_{S,i} = X_{S,i} + \Delta_{u_i}$. We used the synthetic noise approach proposed in [26] to calculate Δ_{u_i} .

D. Aligned and Augmented Adversarial Ensemble (A3E)

We propose A3E to train an accurate and robust EEG classifier for the target user, based on the target domain calibration set $\mathcal{D}_T = \{(X_{T,i}, y_{T,i})\}_{i=1}^{N_T}$. A3E has the following four steps:

- 1) *Data alignment*, where EA is performed on the calibration dataset \mathcal{D}_T . EA first computes the Euclidean arithmetic mean \bar{R} of all N_T spatial covariance matrices:

$$\bar{R} = \frac{1}{N_T} \sum_{i=1}^{N_T} X_{T,i} (X_{T,i})^\top. \quad (1)$$

Then, it performs the alignment by:

$$X_{T,i} \leftarrow \bar{R}^{-1/2} X_{T,i}, \quad i = 1, \dots, N_T. \quad (2)$$

After EA, the EEG trials are whitened, i.e., the average spatial covariance matrix becomes the identity matrix. Since EA is also performed in each source domain, EEG data distributions from different users become more consistent. Note that other alignment approaches, e.g., label alignment [46] and centroid alignment [47], may also be used.

- 2) *Data augmentation*, which increases the diversity of the calibration data. We use data multiplication (Scale) for data augmentation, which scales the amplitude of an EEG trial X by a coefficient close to 1 [48]:

$$X' = X \cdot (1 \pm \beta), \quad X \in \mathcal{D}_T. \quad (3)$$

$\beta = 0.05$ was used in our experiments. After data augmentation, we obtain the augmented calibration set $\mathcal{D}'_T = \{(X_{T,i}, y_{T,i}), (X'_{T,i}, y_{T,i})\}_{i=1}^{N_T}$. Note that other data augmentation approaches, e.g., channel reflection [49], may also be used.

- 3) *Adversarial training*, which generates and uses adversarial samples in training to enhance the classifier robustness and generalization. It can be formulated as a min-max (saddle point) optimization problem:

$$\min_{\theta} \mathbb{E}_{(X_T, y_T) \sim \mathcal{D}'_T} \left[\max_{X_T^{adv} \in \mathcal{B}(X_T, \epsilon)} \mathcal{L}(C_{\theta}(X_T^{adv}), y_T) \right], \quad (4)$$

where $\mathcal{B}(X_T, \epsilon)$ is the ℓ_{∞} ball of radius ϵ centered at X_T , C_{θ} a classifier with parameter θ , and \mathcal{L} its loss function. In this paper, X^{adv} was an adversarial sample generated by projected gradient descent (PGD) [35]. PGD starts from a perturbed version $X^{adv,0}$ of a benign sample X :

$$X^{adv,0} = X + \xi, \quad (5)$$

where ξ is uniform random noise sampled from $(-\epsilon, \epsilon)$. $X^{adv,i}$ is then iteratively updated by:

$$X^{adv,i} = \text{Proj}_{X, \epsilon} (X^{adv,i-1} + \alpha \cdot \text{sign}(\nabla_{X^{adv,i-1}} \mathcal{L}(C_{\theta}(X^{adv,i-1}), y_T))), \quad (6)$$

where $\alpha \leq \epsilon$ is the step size. The function $\text{Proj}_{X, \epsilon}$ ensures that $X^{adv,i}$ remains within the ϵ -neighborhood of X according to the ℓ_{∞} norm.

When a privacy-unlearnable EEG training dataset $\tilde{\mathcal{D}}_S = \{(\tilde{X}_{S,i}, y_{S,i}, u_i)\}_{i=1}^{N_S}$ is given, the optimization problem becomes:

$$\min_{\theta} \mathbb{E}_{(X_T, y_T) \sim \mathcal{D}'_T, (\tilde{X}_S, y_S) \sim \tilde{\mathcal{D}}_S} \left[\max_{X_T^{adv} \in \mathcal{B}(X_T, \epsilon)} \mathcal{L}(C_{\theta}(X_T^{adv}), y_T) + \right] \quad (7)$$

The model is optimized on the normal samples of the source domain and the adversarial samples of the target domain.

- 4) *Ensemble learning*, which aggregates multiple neural networks trained with different random seeds to enhance the classification accuracy and robustness.

The integration of data augmentation and adversarial training enables the classifier to learn a more generalizable classification boundary, as illustrated in Figure 6.

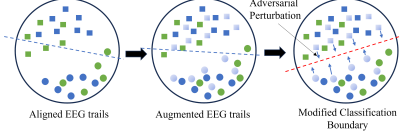


Fig. 6: The impact of data augmentation and adversarial training on the classification boundary.

IV. EXPERIMENT SETTINGS

This section introduces our experiment settings, including the datasets, performance evaluation metrics, and baseline algorithms. Our source code will be made available after this paper is accepted.

A. Datasets

The following three MI datasets, summarized in Table I, were used:

- 1) BNCI2014001 [50], which is Dataset 2a in BCI Competition IV¹. It was collected from 9 subjects. There are four classes, i.e., left hand, right hand, both feet, and tongue. The 22-channel EEG signals were sampled at 256 Hz. Each subject had 144 EEG epochs per class.
- 2) Weibo2014 [51], which was collected from 10 subjects for seven-class classification, i.e., left hand, right hand, both feet, both hands, left hand combined with right foot, right hand combined with left foot, and rest state. The data collection process was divided into 9 sections, with 5 to 10 minutes intersession break. We only used data from the first six classes. The 64-channel EEG signals were sampled at 200 Hz. Each subject had 80 EEG epochs per class.
- 3) BNCI2014002 [52], which was collected from 14 subjects for left hand and right hand MI classification. The 15-channel EEG signals were sampled at 250 Hz. Each subject had 80 EEG epochs per class.

TABLE I: Summary of three datasets.

Dataset	# of Subjects	# of Time Samples	# of Channels	# of Trials per Subject	# of Classes
BNCI2014001	9	512	22	576	4
Weibo2014	10	512	64	480	6
BNCI2014002	14	512	15	160	2

For all three datasets, we extracted the EEG data in [0, 4] seconds after each imagination prompt, band-pass filtered the trials at [8, 32] Hz, and resampled the data to 128 Hz.

B. Performance Evaluation Metrics

We computed the classification accuracies on benign, adversarial, and noisy samples for primary performance evaluation. PGD [27], calculated by (5) and (6), was used to generate adversarial samples.

Given an EEG trial X , the noisy sample X' was calculated as:

$$X' = X + \eta \cdot \sigma(X) \cdot U(-1, 1), \quad (8)$$

where $U(-1, 1) \in \mathbb{R}^{c \times t}$ is a noise matrix whose each element is a uniformly distributed number in $[-1, 1]$. $\sigma(X)$ denotes the vector composed of the standard deviations of each channel in X :

$$\sigma(X) = [\sigma(X(1)), \sigma(X(2)), \dots, \sigma(X(c))]', \quad (9)$$

where $\sigma(X(1))$ denotes the standard deviation of the first channel in X .

Additionally, to comprehensively evaluate the robustness of the classifiers, we computed their mean accuracies on samples with different perturbation magnitudes. For adversarial samples, we computed the classification accuracies on samples with adversarial perturbation magnitudes $\epsilon = \{0.01, 0.03, 0.05\}$ times the standard deviation of the original sample channels. For noisy samples, we computed the classification accuracies on samples with noise perturbation magnitudes $\eta = \{1, 2, 3\}$ times the standard deviation of the original sample channels. We repeated each experiment five times, and report their averages.

Figure 7 shows a benign EEG sample, its PGD counterpart with perturbation magnitude $\epsilon = 0.01$, and its noisy counterpart with perturbation magnitude $\eta = 1$. The adversarial perturbation and the random noise differ significantly. Although the adversarial sample closely resembles the benign sample, it can still lead to a substantial drop in EEG classification performance.

C. Baseline Algorithms

We compared our proposed A3E with the following 13 algorithms in the literature:

- 1) Common spatial pattern (CSP) [53], a classic MI classification approach. It uses labelled data to design spatial filters and performs feature extraction and Linear Discriminant Analysis (LDA) classification. The labelled data could be from the source domain only (S), the target domain only (T), or source and target domains combined (S&T).
- 2) EEGNet [54], a popular compact end-to-end convolutional neural network for EEG signal decoding. The labeled source and target data are combined in mini-batch gradient descent training. One variant is to sample each mini-batch randomly (usually there are more source samples than target samples in each mini-batch), referred to as S&T. Another variant is to sample a half-batch from each domain and then combine them into a full mini-batch (this ensures an equal number of samples from both domains), referred to as S+T.

¹<https://www.bbc.de/competition/iv/>

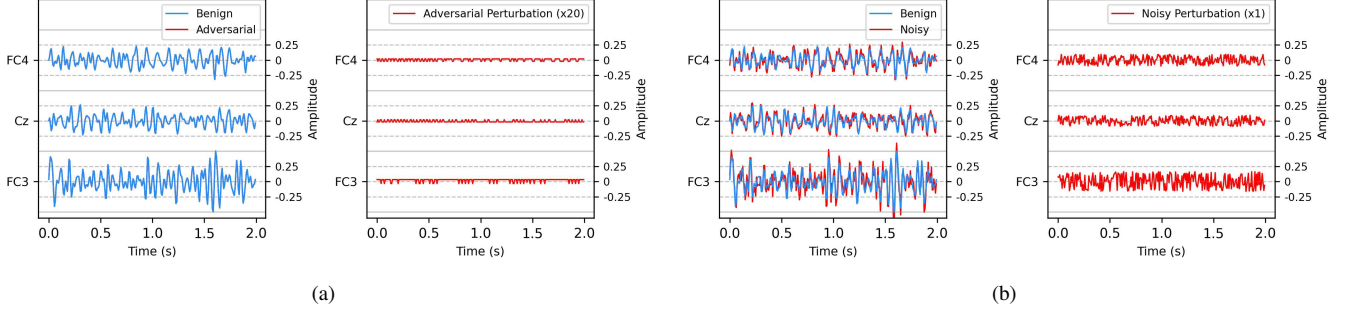


Fig. 7: A benign EEG sample and the corresponding (a) PGD adversarial sample; and, (b) Noisy sample.

- 3) Deep domain adaptation approaches, including ENT [55], DANN [30], JAN [31], CDAN [34], DAN [29], MME [56], MDD [33], MCC [32], SHOT [25], and CC [57], all with EEGNet backbone. In model training and fine-tuning, we used Cross-Entropy (CE) loss plus the losses from these specific domain adaptation approaches, whose weights were all set to 1. DANN, JAN, CDAN, DAN and MDD, whose calculations need source data, were not performed in centralized source-free transfer learning and federated source-free transfer learning scenarios.
- 4) ABAT [27], which leverages data alignment and adversarial training to simultaneously enhances the model's accuracy on both benign and adversarial samples.

For fair comparison, we also report the performance of ABAT ensemble (ABAT-E) and non-ensemble A3E (A3) in Section V. The robust training perturbation amplitude ϵ in ABAT, ABAT-E, A3 and A3E were all set to 0.03 [27]. (1) and (2) were used in all experiments to align the source data and the target calibration data for improved performance. In the test phase, we aligned the test data with the Euclidean arithmetic mean \bar{R} calculated on the target domain calibration set, to avoid data leakage.

V. RESULTS

This section presents experimental results to demonstrate the effectiveness of our proposed approach in three privacy protection scenarios.

A. Centralized Source-Free Transfer Learning Scenario

All source models were pre-trained in the centralized source-free transfer learning scenario, and then fine-tuned using the first 20%, 30%, 40%, 50% and 60% of the target user's data as the calibration set. The average model accuracies are shown in Table II, and the detailed accuracies are shown in Figure 8.

Table II shows that the average accuracies of the four robust training approaches (ABAT, ABAT-E, A3, and A3E) on three types of samples (benign, adversarial, and noisy) were higher than the other 10 approaches across the three datasets. Additionally, their rank was consistently $ABAT < ABAT-E < A3 < A3E$, demonstrating the effectiveness of our proposed approaches.

Figure 8 shows that:

- 1) As the amount of training data increased, the accuracies of the four robust training approaches (ABAT, ABAT-E, A3, and A3E) exhibited a clear upward trend across all sample types. In most cases, A3E achieved the highest classification accuracy, and A3 the second highest, demonstrating again the effectiveness of our proposed approaches.
- 2) For EEGNet(T) and various domain adaptation algorithms, increasing the amount of training data also led to noticeable accuracy improvements on benign and noisy samples. However, the accuracy on adversarial samples, i.e., adversarial robustness, may not improve much.

B. Baseline Performance in Centralized Source-Free Machine Learning

The classification accuracies of various baseline approaches on the benign samples are shown in the 'Benign' columns of Table II and the 'Benign' subfigures of Figure 8. Domain adaptation approaches significantly outperformed models trained on the source or target data only. On average, domain adaptation approaches achieved a minimum accuracy of 64.85%, whereas the highest accuracy for models without adaptation was 56.63%. Most domain adaptation losses enhanced the classification accuracy on the benign target samples (with average accuracies over 66.26%), compared to the CE loss only, demonstrating the effectiveness of domain adaptation.

The classification accuracies of various baseline approaches on adversarial and noisy samples are shown in the 'Adversarial' and 'Noisy' columns of Table II, and the 'Adversarial' and 'Noisy' subfigures of Figure 8. Observe that:

- 1) In all cases, classification accuracies on adversarial and noisy samples were significantly lower than those on benign samples, indicating the vulnerability of the classifiers.
- 2) In most cases, domain adaptation approaches achieved better robustness than those trained solely on the source or target domain data, achieving higher accuracies on adversarial and noisy samples.
- 3) On adversarial samples, traditional CSP models outperformed deep EEGNet models and domain adaptation approaches. However, on noisy samples, deep EEGNet models outperformed traditional CSP models.

TABLE II: Classification accuracies (%) in centralized source-free transfer learning. ‘Avg.’ column stands for the average of ‘Benign’, ‘Adversarial’ and ‘Noisy’. ‘Average’ stands for the average results on BNCI2014001, Weibo2014 and BNCI2014002. The highest accuracies in each column are marked in bold.

	BNCI2014001				Weibo2014				BNCI2014002				Average			
	Benign	Adversarial	Noisy	Avg.	Benign	Adversarial	Noisy	Avg.	Benign	Adversarial	Noisy	Avg.	Benign	Adversarial	Noisy	Avg.
CSP(S)	48.31	33.08	31.07	37.49	35.46	21.11	31.91	29.49	70.19	55.75	58.64	61.52	51.32	36.65	40.54	42.83
CSP(T)	55.12	36.61	30.80	40.84	40.85	21.25	24.66	28.92	73.93	54.71	59.70	62.78	56.63	37.52	38.39	44.18
EEGNet(S)	50.99	17.31	34.90	34.40	43.18	12.90	38.14	31.41	72.62	41.02	69.58	61.07	55.60	23.74	47.54	42.29
EEGNet(T)	53.99	20.58	40.02	38.20	38.56	5.65	28.99	24.40	74.44	45.84	65.61	61.96	55.66	24.02	44.87	41.52
CE	62.78	22.97	38.15	41.30	59.18	17.60	47.47	41.42	76.81	47.86	72.23	65.64	66.26	29.48	52.62	49.45
ENT	63.45	25.17	38.88	42.50	59.39	18.30	47.88	41.86	77.67	51.66	73.34	67.56	66.84	31.71	53.37	50.64
MME	61.94	21.84	39.73	41.17	57.00	14.97	45.07	39.01	75.62	45.29	70.93	63.95	64.85	27.37	51.91	48.04
SHOT	63.18	24.28	38.43	41.96	59.47	18.27	47.74	41.83	77.50	50.61	73.07	67.06	66.72	31.05	53.08	50.28
CC	63.42	24.92	38.88	42.41	59.43	18.19	47.80	41.81	77.74	51.49	73.30	67.51	66.87	31.53	53.33	50.58
CC	63.22	24.38	38.47	42.02	59.40	18.46	47.64	41.84	77.56	50.69	73.07	67.11	66.73	31.18	53.06	50.32
ABAT	61.51	39.12	42.74	47.79	62.86	41.72	54.09	52.89	75.61	60.11	73.33	69.69	66.66	46.98	56.72	56.79
ABAT-E	62.99	43.22	42.91	49.71	64.71	45.61	55.44	55.25	76.48	62.01	74.16	70.88	68.06	50.28	57.50	58.62
A3	66.55	45.81	51.50	54.62	64.94	45.51	57.14	55.86	77.87	64.89	75.69	72.82	69.79	52.07	61.45	61.10
A3E	68.76	49.64	52.37	56.92	66.96	49.23	58.94	58.37	78.64	66.89	76.29	73.94	71.45	55.25	62.53	63.08

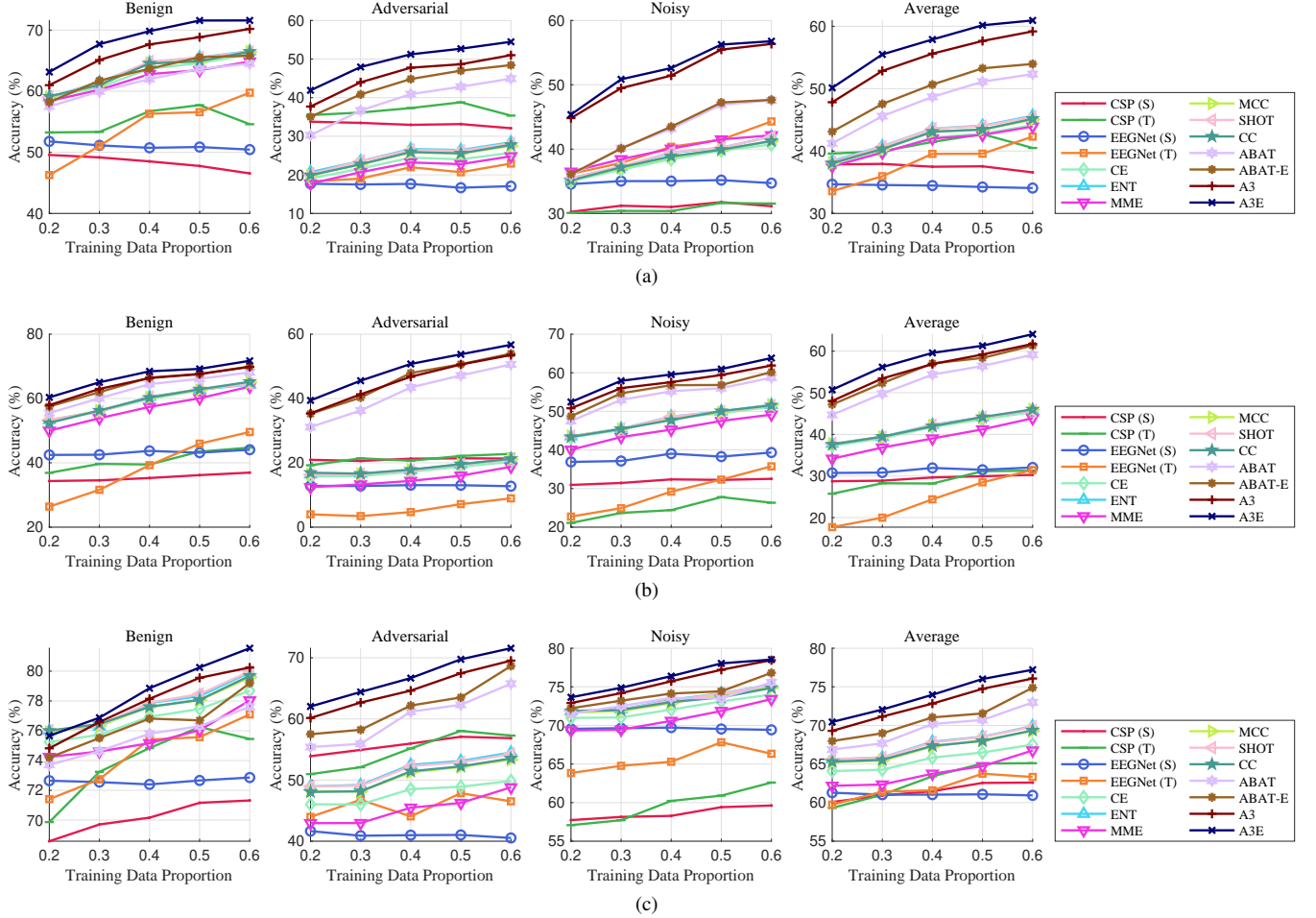


Fig. 8: Classification accuracies (%) in centralized source-free transfer learning for different training data proportions. ‘Average’ stands for the average of ‘Benign’, ‘Adversarial’ and ‘Noisy’. (a) BNCI2014001; (b) Weibo2014; and, (c) BNCI2014002.

C. Federated Source-Free Transfer Learning Scenario

The first 20%, 30%, 40%, 50% and 60% of the target data were used as the calibration set in fine-tuning. All source models, except for the traditional CSP model, were pre-trained using federated source-free transfer learning. The average classification accuracies are shown in Table III, and the detailed accuracies are shown in Figure 9.

Table III shows that, similar to in the centralized source-free transfer learning scenario, the average accuracies of the four robust training approaches (ABAT, ABAT-E, A3, and A3E) were always higher than the other 10 approaches, and the rank was consistently $ABAT < ABAT-E < A3 < A3E$. Figure 9 shows that A3E was always the best-performing approach.

A comparison of the performance of EEGNet(S) in Tables II and III reveals that the source models trained in federated source-free transfer learning outperformed those trained in centralized source-free transfer learning. Additionally, after fine-tuning on the target domain calibration set, models pre-trained in federated transfer achieved significantly better performance on adversarial and noisy samples, compared to those pre-trained in centralized transfer. This may be due to the following reasons:

- 1) The EEG data distribution differs significantly across users. In federated transfer, calculating Batch Normalization (BN) parameters for each user individually during model training allows the network to learn more robust global task information, compared to computing a single set of BN parameters for all source data in centralized transfer.
- 2) Using batch-specific BN parameters during testing leads to better adaptation to the test data, resulting in improved robustness.

D. Source Data Perturbation Scenario

We combined the perturbed source data with the first 20%, 30%, 40%, 50% and 60% of the target data in training. The average classification accuracies are shown in Table IV, and the detailed accuracies in Figure 10.

Table IV also reveals that:

- 1) The four robust training approaches (ABAT, ABAT-E, A3, and A3E) again demonstrated better performance than others, and their rank was $ABAT \approx A3 < ABAT-E \approx A3E$. The utilization of source EEG data reduced performance difference between ABAT and A3; however, ensemble learning still achieved further performance improvement.
- 2) For the CSP model, mixing source and target data (S&T) did not always enhance the performance, compared to training on source or target data alone. This may indicate that traditional models are more affected by domain distribution discrepancies, limiting their ability to capture shared features. In contrast, EEGNet performed better with mixed source and target data.

The classification accuracies on the benign samples are shown in the ‘Benign’ columns of Table IV and the ‘Benign’ subfigures of Figure 10. Compared to models trained only on source or target domain data, or on a mix of the two (S&T),

domain adaptation algorithms notably improved the accuracies on benign target domain samples. Different domain adaptation losses did not significantly enhance accuracies over S+T on benign samples. This may be because mixing source and target data within each batch (S+T) enabled models to learn sufficient cross-domain knowledge, so further adaptation to the target data yielded limited benefit.

Tables II-IV show that training with perturbed source data plus the target calibration data yielded higher classification accuracies on benign samples, e.g., the highest average accuracy on benign samples in Table IV is 73.49%, surpassing 71.45% in Table II and 71.93% in Table III.

E. Comparison with Approaches without Privacy Protection

To further verify the performance of our proposed A3E, we combined the source domain data and the first 20%, 30%, 40%, 50% and 60% target domain data for model training, without imposing any privacy protection strategy. The average classification accuracies are shown in Table V, and the detailed accuracies are shown in Figure 11. The four robust training approaches again achieved the highest accuracies.

VI. CONCLUSIONS

This paper has proposed an A3E approach, which leverages data alignment, data augmentation, adversarial training and ensemble learning to achieve more accurate and more robust EEG decoding. A3E is then integrated into three privacy protection scenarios (centralized source-free transfer, federated source-free transfer, and source data perturbation) to achieve simultaneously accurate classification, adversarial robustness, and privacy protection. Experiments on three public MI datasets demonstrated the effectiveness of A3E, even outperforming state-of-the-art transfer learning approaches that do not consider privacy protection at all. This is the first time that three major challenges in EEG-based BCIs (data scarcity and individual differences, adversarial vulnerability, and user privacy) can be accommodated simultaneously, significantly improving the practicalness of EEG decoding algorithms in real-world BCIs.

REFERENCES

- [1] M. Ienca, P. Haselager, and E. J. Emanuel, “Brain leaks and consumer neurotechnology,” *Nature Biotechnology*, vol. 36, no. 9, pp. 805–810, 2018.
- [2] J. J. Daly and J. R. Wolpaw, “Brain-computer interfaces in neurological rehabilitation,” *The Lancet Neurology*, vol. 7, no. 11, pp. 1032–1043, 2008.
- [3] J. E. O’Doherty, M. A. Lebedev, P. J. Ifft, K. Z. Zhuang, S. Shokur, H. Bleuler, and M. A. L. Nicolelis, “Active tactile exploration using a brain-machine-brain interface,” *Nature*, vol. 479, no. 7372, pp. 228–231, 2011.
- [4] L. R. Hochberg, D. Bacher, B. Jarosiewicz, N. Y. Masse, J. D. Simeral, J. Vogel, S. Haddadin, J. Liu, S. S. Cash, P. Van Der Smagt *et al.*, “Reach and grasp by people with tetraplegia using a neurally controlled robotic arm,” *Nature*, vol. 485, no. 7398, pp. 372–375, 2012.
- [5] S. L. Metzger, K. T. Littlejohn, A. B. Silva, D. A. Moses, M. P. Seaton, R. Wang, M. E. Dougherty, J. R. Liu, P. Wu, M. A. Berger, I. Zhuravleva, A. Tu-Chan, K. Ganguly, G. K. Anumanchipalli, and E. F. Chang, “A high-performance neuroprosthesis for speech decoding and avatar control,” *Nature*, vol. 7976, no. 620, pp. 1037–1046, 2023.
- [6] L. F. Nicolas-Alonso and J. Gomez-Gil, “Brain computer interfaces, a review,” *Sensors*, vol. 12, no. 2, pp. 1211–1279, 2012.

TABLE III: Classification accuracies (%) in federated source-free transfer learning scenario. ‘Avg.’ column stands for the average of ‘Benign’, ‘Adversarial’ and ‘Noisy’. ‘Average’ stands for the average results on BNCI2014001, Weibo2014 and BNCI2014002. The highest accuracies in each column are marked in bold.

	BNCI2014001				Weibo2014				BNCI2014002				Average			
	Benign	Adversarial	Noisy	Avg.	Benign	Adversarial	Noisy	Avg.	Benign	Adversarial	Noisy	Avg.	Benign	Adversarial	Noisy	Avg.
CSP(S)	48.31	33.08	31.07	37.49	35.46	21.11	31.91	29.49	70.19	55.75	58.64	61.52	51.32	36.65	40.54	42.83
CSP(T)	55.12	36.61	30.80	40.84	40.85	21.25	24.66	28.92	73.93	54.71	59.70	62.78	56.63	37.52	38.39	44.18
EEGNet(S)	51.49	20.26	48.24	40.00	49.64	16.72	46.52	37.63	74.63	47.95	72.57	65.05	58.58	28.31	55.78	47.56
EEGNet(T)	53.99	20.58	40.02	38.20	38.56	5.65	28.99	24.40	74.44	45.84	65.61	61.96	55.66	24.02	44.87	41.52
CE	61.68	34.50	57.93	51.37	59.50	24.16	55.66	46.44	79.75	60.57	77.60	72.64	66.98	39.74	63.73	56.82
ENT	57.49	34.71	54.77	48.99	53.15	25.12	50.44	42.90	79.63	61.85	77.54	73.01	63.42	40.56	60.92	54.97
MME	62.26	33.46	58.34	51.35	60.27	22.29	55.95	46.17	78.90	59.36	76.75	71.67	67.14	38.37	63.68	56.40
MCC	61.25	34.61	57.59	51.15	59.27	24.52	55.57	46.45	79.75	61.11	77.69	72.85	66.76	40.08	63.62	56.82
SHOT	59.46	34.77	56.22	50.15	57.32	25.58	54.26	45.72	79.85	61.71	77.70	73.09	65.54	40.69	62.72	56.32
CC	61.12	34.57	57.52	51.07	59.26	24.51	55.52	46.43	79.83	61.16	77.67	72.89	66.74	40.08	63.57	56.80
ABAT	59.67	43.34	57.42	53.47	60.65	46.24	58.28	55.06	78.42	65.18	77.04	73.55	66.25	51.58	64.25	60.69
ABAT-E	61.99	47.47	59.46	56.31	63.18	49.89	60.32	57.80	79.19	67.30	77.90	74.80	68.12	54.89	65.90	62.97
A3	65.26	48.93	62.54	58.91	64.41	49.06	61.64	58.37	80.88	69.35	79.44	76.56	70.18	55.78	67.87	64.61
A3E	67.45	51.95	64.65	61.35	66.72	52.39	63.55	60.89	81.62	70.63	80.28	77.51	71.93	58.32	69.49	66.58

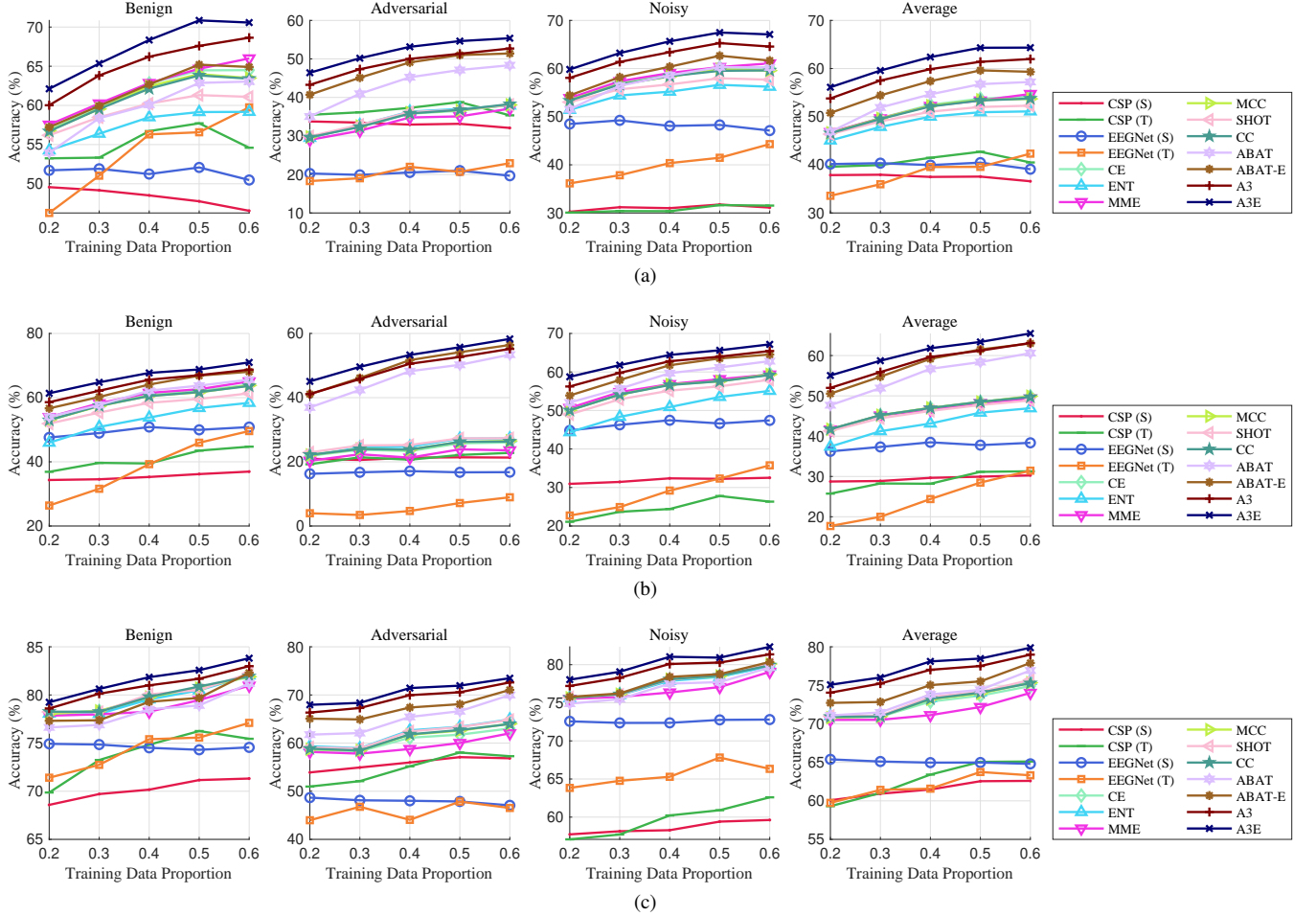


Fig. 9: Classification accuracies (%) in federated source-free transfer learning for different training data proportions. ‘Average’ stands for the average of ‘Benign’, ‘Adversarial’ and ‘Noisy’. (a) BNCI2014001; (b) Weibo2014; and, (c) BNCI2014002.

TABLE IV: Classification accuracies (%) in source data perturbation. ‘Avg.’ column stands for the average of ‘Benign’, ‘Adversarial’ and ‘Noisy’. ‘Average’ stands for the average results on BNCI2014001, Weibo2014 and BNCI2014002. The highest accuracies in each column are marked in bold.

	BNCI2014001				Weibo2014				BNCI2014002				Average			
	Benign	Adversarial	Noisy	Avg.	Benign	Adversarial	Noisy	Avg.	Benign	Adversarial	Noisy	Avg.	Benign	Adversarial	Noisy	Avg.
CSP(S)	48.31	33.08	31.07	37.49	35.46	21.11	31.91	29.49	70.19	55.75	58.64	61.52	51.32	36.65	40.54	42.83
CSP(T)	55.12	36.61	30.80	40.84	40.85	21.25	24.66	28.92	73.93	54.71	59.70	62.78	56.63	37.52	38.39	44.18
CSP(S&T)	49.49	32.94	31.91	38.11	37.59	20.59	32.72	30.30	69.14	55.28	60.77	61.73	52.07	36.27	41.80	43.38
EEGNet(S)	50.99	17.31	34.90	34.40	43.18	12.90	38.14	31.41	72.62	41.02	69.58	61.07	55.60	23.74	47.54	42.29
EEGNet(T)	53.99	20.58	40.02	38.20	38.56	5.65	28.99	24.40	74.44	45.84	65.61	61.96	55.66	24.02	44.87	41.52
EEGNet(S&T)	56.22	23.01	37.74	38.99	49.85	18.04	42.48	36.79	75.68	48.47	71.45	65.20	60.58	29.84	50.56	46.99
S+T	68.37	30.69	43.11	47.39	58.98	17.65	50.47	42.37	79.51	52.48	74.35	68.78	68.95	33.60	55.98	52.84
ENT	66.83	29.95	44.14	46.97	50.08	11.62	42.74	34.81	77.28	52.59	72.07	67.31	64.73	31.39	52.98	49.70
DANN	63.84	23.00	41.78	42.87	55.78	14.76	49.02	39.85	77.25	47.82	72.69	65.92	65.62	28.53	54.49	49.55
JAN	61.81	31.86	44.57	46.08	59.47	19.71	51.96	43.71	73.22	54.30	70.41	65.98	64.83	35.29	55.65	51.92
CDAN	67.41	29.60	43.28	46.76	58.73	17.49	50.77	42.33	79.01	51.48	74.10	68.20	68.38	32.86	56.05	52.43
DAN	66.37	29.67	43.92	46.65	58.89	17.83	50.91	42.54	75.69	52.12	71.51	66.44	66.98	33.21	55.45	51.88
MME	65.32	31.25	45.81	47.46	51.87	14.18	44.64	36.90	79.34	55.61	74.77	69.91	65.51	33.68	55.07	51.42
MDD	68.37	30.84	43.47	47.56	58.83	17.41	50.22	42.15	79.18	52.09	74.42	68.56	68.79	33.44	56.04	52.76
MCC	68.12	32.15	45.14	48.47	54.00	14.45	46.36	38.27	79.44	52.85	73.91	68.73	67.19	33.15	55.14	51.83
SHOT	65.28	29.43	43.66	46.13	48.42	11.15	40.96	33.51	79.08	51.73	73.92	68.25	64.26	30.77	52.85	49.29
CC	67.91	31.19	46.37	48.49	53.17	12.89	45.91	37.32	79.18	52.00	74.57	68.58	66.75	32.03	55.62	51.46
ABAT	69.59	48.04	48.90	55.51	64.79	43.31	56.74	54.95	79.94	62.39	76.93	73.09	71.44	51.24	60.86	61.18
ABAT-E	71.12	51.97	49.42	57.51	68.57	48.83	60.61	59.34	80.78	65.35	77.84	74.66	73.49	55.39	62.62	63.83
A3	69.59	47.73	50.95	56.09	63.50	42.27	56.50	54.09	80.03	62.11	76.97	73.04	71.04	50.71	61.47	61.07
A3E	71.34	51.92	51.76	58.34	67.77	47.76	60.64	58.73	80.76	65.41	77.98	74.72	73.29	55.03	63.46	63.93

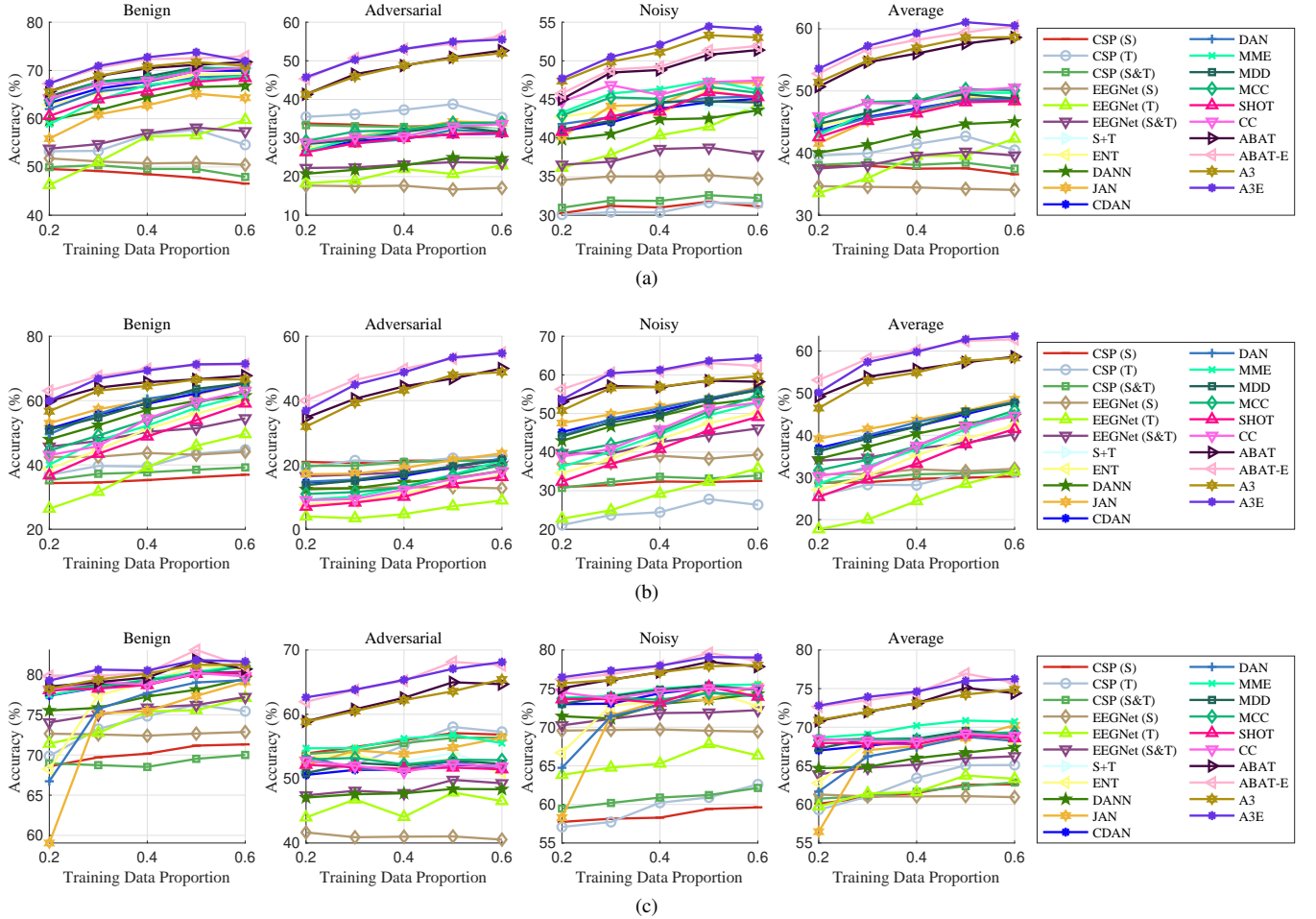


Fig. 10: Classification accuracies (%) in source data perturbation for different training data proportions. ‘Average’ stands for the average of ‘Benign’, ‘Adversarial’ and ‘Noisy’. (a) BNCI2014001; (b) Weibo2014; and, (c) BNCI2014002.

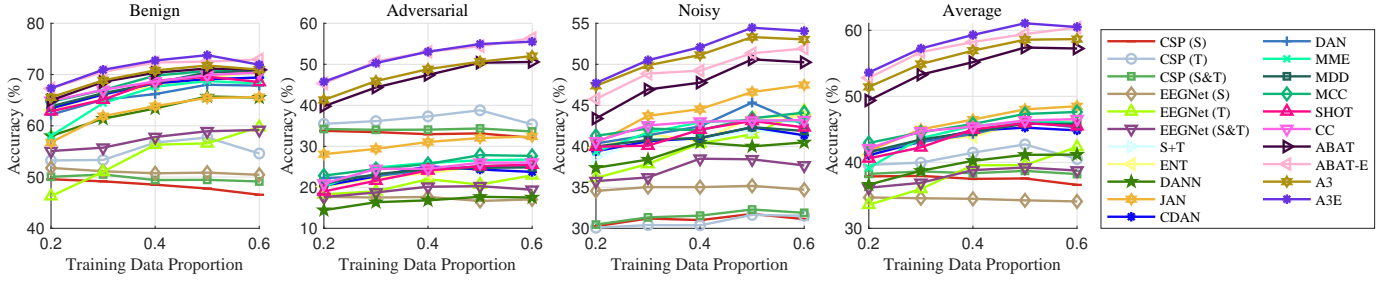


Fig. 11: Classification accuracies (%) without privacy protection, with different training data proportions. ‘Average’ stands for the average of ‘Benign’, ‘Adversarial’ and ‘Noisy’.

TABLE V: Classification accuracies (%) without privacy protection. ‘Average’ column stands for the average of ‘Benign’, ‘Adversarial’ and ‘Noisy’. The highest accuracies in each column are marked in bold.

	BNCI2014001			
	Benign	Adversarial	Noisy	Average
CSP(S)	48.31	33.08	31.07	37.49
CSP(T)	55.12	36.61	30.80	40.84
CSP(S&T)	49.71	34.05	31.50	38.42
EEGNet(S)	50.99	17.31	34.90	34.40
EEGNet(T)	53.99	20.58	40.02	38.20
EEGNet(S&T)	57.35	19.24	37.31	37.96
S+T	67.60	23.85	40.73	44.06
ENT	67.37	23.29	41.82	44.16
DANN	62.80	16.56	39.34	39.57
JAN	62.71	30.58	44.53	45.94
CDAN	67.26	23.26	40.93	43.82
DAN	65.86	23.94	42.42	44.07
MME	65.41	24.86	42.03	44.10
MDD	67.92	23.63	41.19	44.25
MCC	68.65	25.70	42.58	45.64
SHOT	66.97	23.08	41.49	43.85
CC	68.16	24.39	42.50	45.02
ABAT	69.19	46.50	47.78	54.49
ABAT-E	70.75	50.54	48.21	56.50
A3	69.55	46.53	49.80	55.30
A3E	71.10	50.75	50.46	57.43

- [7] G. Pfurtscheller and C. Neuper, “Motor imagery and direct brain-computer communication,” *Proc. of the IEEE*, vol. 89, no. 7, pp. 1123–1134, 2001.
- [8] D. Wu, X. Jiang, and R. Peng, “Transfer learning for motor imagery based brain-computer interfaces: A tutorial,” *Neural Networks*, vol. 153, pp. 235–253, 2022.
- [9] X. Zhang and D. Wu, “On the vulnerability of CNN classifiers in EEG-based BCIs,” *IEEE Trans. on Neural Systems and Rehabilitation Engineering*, vol. 27, no. 5, pp. 814–825, 2019.
- [10] X. Zhang, D. Wu, L. Ding, H. Luo, C.-T. Lin, T.-P. Jung, and R. Chavarriaga, “Tiny noise, big mistakes: Adversarial perturbations induce errors in brain-computer interface spellers,” *National Science Review*, vol. 8, no. 4, p. nwaa233, 2021.
- [11] Z. Liu, L. Meng, X. Zhang, W. Fang, and D. Wu, “Universal adversarial perturbations for CNN classifiers in EEG-based BCIs,” *Journal of Neural Engineering*, vol. 18, no. 4, p. 0460a4, 2021.
- [12] X. Wang, R. O. S. Quintanilla, M. Hersche, L. Benini, and G. Singh, “Physically-constrained adversarial attacks on brain-machine interfaces,” in *Proc. Workshop on Trustworthy and Socially Responsible Machine Learning*, Dec. 2022, Online.
- [13] R. Bian, L. Meng, and D. Wu, “SSVEP-based brain-computer interfaces are vulnerable to square wave attacks,” *Science China Information Sciences*, vol. 65, no. 4, pp. 1–13, 2022.
- [14] J. Jung, H. Moon, G. Yu, and H. Hwang, “Generative perturbation network for universal adversarial attacks on brain-computer interfaces,” *IEEE Journal of Biomedical and Health Informatics*, vol. 27, no. 11, pp. 5622–5633, 2023.
- [15] L. Meng, X. Jiang, X. Chen, W. Liu, H. Luo, and D. Wu, “Adversarial filtering based evasion and backdoor attacks to EEG-based brain-computer interfaces,” *Information Fusion*, vol. 107, p. 102316, 2024.
- [16] R. Gunawardena, S. Jayawardena, S. Seneviratne, R. Masood, and S. S. Kanhere, “Single-sensor sparse adversarial perturbation attacks against behavioural biometrics,” *IEEE Internet of Things Journal*, vol. 11, no. 16, pp. 27 303–27 321, 2024.
- [17] L. Meng, C.-T. Lin, T.-P. Jung, and D. Wu, “White-box target attack for EEG-based BCI regression problems,” in *Proc. Int’l Conf. on Neural Information Processing*, Sydney, Australia, Dec. 2019, pp. 476–488.
- [18] S. Zhang, L. Sun, X. Mao, C. Hu, and P. Liu, “Review on EEG-based authentication technology,” *Computational intelligence and neuroscience*, vol. 2021, no. 1, p. 5229576, 2021.
- [19] K. Xia, W. Duch, Y. Sun, K. Xu, W. Fang, H. Luo, Y. Zhang, D. Sang, X. Xu, F.-Y. Wang, and D. Wu, “Privacy-preserving brain-computer interfaces: A systematic review,” *IEEE Trans. on Computational Social Systems*, vol. 10, no. 5, pp. 2312–2324, 2023.
- [20] I. Martinovic, D. Davies, M. Frank, D. Perito, T. Ros, and D. Song, “On the feasibility of side-channel attacks with brain-computer interfaces,” in *Proc. 21st USENIX Security Symposium (USENIX Security 12)*, Bellevue, WA, Aug. 2012, pp. 143–158.
- [21] O. Landau, A. Cohen, S. Gordon, and N. Nissim, “Mind your privacy: Privacy leakage through BCI applications using machine learning methods,” *Knowledge-Based Systems*, vol. 198, p. 105932, 2020.
- [22] H. He and D. Wu, “Transfer learning for brain-computer interfaces: A Euclidean space data alignment approach,” *IEEE Trans. on Biomedical Engineering*, vol. 67, no. 2, pp. 399–410, 2019.
- [23] L. Meng, X. Jiang, and D. Wu, “Adversarial robustness benchmark for EEG-based brain-computer interfaces,” *Future Generation Computer System*, vol. 143, pp. 231–247, 2023.
- [24] X. Chen, L. Meng, Y. Xu, and D. Wu, “Adversarial artifact detection in EEG-based brain-computer interfaces,” *Journal of Neural Engineering*, vol. 21, no. 5, p. 056043, 2024.
- [25] J. Liang, D. Hu, Y. Wang, R. He, and J. Feng, “Source data-absent unsupervised domain adaptation through hypothesis transfer and labeling transfer,” *IEEE Trans. on Pattern Analysis and Machine Intelligence*, vol. 44, no. 11, pp. 8602–8617, 2022.
- [26] X. Chen, S. Li, Y. Tu, Z. Wang, and D. Wu, “User-wise perturbations for user identity protection in EEG-based BCIs,” *Journal of Neural Engineering*, 2024, in press.
- [27] X. Chen, Z. Wang, and D. Wu, “Alignment-based adversarial training (ABAT) for improving the robustness and accuracy of EEG-based BCIs,” *IEEE Trans. on Neural Systems and Rehabilitation Engineering*, vol. 32, pp. 1703–1714, 2024.
- [28] K. Xia, L. Deng, W. Duch, and D. Wu, “Privacy-preserving domain adaptation for motor imagery-based brain-computer interfaces,” *IEEE Trans. on Biomedical Engineering*, pp. 3365–3376, 2022.
- [29] M. Long, Y. Cao, Z. Cao, J. Wang, and M. I. Jordan, “Transferable representation learning with deep adaptation networks,” *IEEE Trans. on Pattern Analysis and Machine Intelligence*, vol. 41, no. 12, pp. 3071–3085, 2019.
- [30] Y. Ganin, E. Ustinova, H. Ajakan, P. Germain, H. Larochelle, F. Laviolette, M. Marchand, and V. Lempitsky, “Domain-adversarial training of neural networks,” *The Journal of Machine Learning Research*, vol. 17, no. 1, pp. 2096–2030, 2016.
- [31] M. Long, H. Zhu, J. Wang, and M. I. Jordan, “Deep transfer learning with joint adaptation networks,” in *Proc. Int’l Conf. on Machine Learning*, vol. 70, Aug. 2017, pp. 2208–2217.
- [32] Y. Jin, X. Wang, M. Long, and J. Wang, “Minimum class confusion

- for versatile domain adaptation,” in *Proc. European Conf. on Computer Vision*, Glasgow, UK, Aug. 2020, pp. 464–480.
- [33] Y. Zhang, T. Liu, M. Long, and M. Jordan, “Bridging theory and algorithm for domain adaptation,” in *Proc. Int’l Conf. on Machine Learning*, vol. 97, Jun 2019, pp. 7404–7413.
- [34] M. Long, Z. Cao, J. Wang, and M. I. Jordan, “Conditional adversarial domain adaptation,” in *Proc. Int’l Conf. on Neural Information Processing Systems*, Red Hook, NY, Dec. 2018, pp. 1647–1657.
- [35] A. Madry, A. Makelov, L. Schmidt, D. Tsipras, and A. Vladu, “Towards deep learning models resistant to adversarial attacks,” in *Proc. Int’l Conf. on Learning Representations*, Vancouver, Canada, Apr. 2018, pp. 1–28.
- [36] X. Chen, C. Li, A. Liu, M. J. McKeown, R. Qian, and Z. J. Wang, “Toward open-world electroencephalogram decoding via deep learning: A comprehensive survey,” *IEEE Signal Processing Magazine*, vol. 39, no. 2, pp. 117–134, 2022.
- [37] H. Zhang, Y. Yu, J. Jiao, E. Xing, L. El Ghaoui, and M. Jordan, “Theoretically principled trade-off between robustness and accuracy,” in *Proc. Int’l Conf. on Machine Learning*, Long Beach, CA, Jun. 2019, pp. 7472–7482.
- [38] S. Zhang, Z. Qian, K. Huang, Q. Wang, R. Zhang, and X. Yi, “Towards better robust generalization with shift consistency regularization,” in *Proc. Int’l Conf. on Machine Learning*, Jul. 2021, pp. 12 524–12 534, Online.
- [39] B. Xue, L. Wu, A. Liu, X. Zhang, X. Chen, and X. Chen, “Detecting the universal adversarial perturbations on high-density sEMG signals,” *Computers in biology and medicine*, vol. 149, p. 105978, 2022.
- [40] D. Wu, W. Fang, Y. Zhang, L. Yang, X. Xu, H. Luo, and X. Yu, “Adversarial attacks and defenses in physiological computing: A systematic review,” *National Science Open*, vol. 2, no. 1, 2023.
- [41] Y. Li, X. Yu, S. Yu, and B. Chen, “Adversarial training for the adversarial robustness of EEG-based brain-computer interfaces,” in *Proc. IEEE Int’l Workshop on Machine Learning for Signal Processing (MLSP)*, Xian, China, Aug. 2022, pp. 1–6.
- [42] W. Zhang, Z. Wang, and D. Wu, “Multi-source decentralized transfer for privacy-preserving BCIs,” *IEEE Trans. on Neural Systems and Rehabilitation Engineering*, vol. 30, pp. 2710–2720, 2022.
- [43] W. Zhang and D. Wu, “Lightweight source-free transfer for privacy-preserving motor imagery classification,” *IEEE Trans. on Cognitive and Developmental Systems*, vol. 15, no. 2, pp. 938–949, 2023.
- [44] T. Jia, L. Meng, S. Li, J. Liu, and D. Wu, “Federated motor imagery classification for privacy-preserving brain-computer interfaces,” *IEEE Trans. on Neural Systems and Rehabilitation Engineering*, vol. 32, pp. 3442–3451, 2024.
- [45] L. Meng, X. Jiang, J. Huang, Z. Zeng, S. Yu, T.-P. Jung, C.-T. Lin, R. Chavarriaga, and D. Wu, “EEG-based brain-computer interfaces are vulnerable to backdoor attacks,” *IEEE Trans. on Neural Systems and Rehabilitation Engineering*, vol. 31, pp. 2224–2234, 2023.
- [46] H. He and D. Wu, “Different set domain adaptation for brain-computer interfaces: A label alignment approach,” *IEEE Trans. on Neural Systems and Rehabilitation Engineering*, vol. 28, no. 5, pp. 1091–1108, 2020.
- [47] W. Zhang and D. Wu, “Manifold embedded knowledge transfer for brain-computer interfaces,” *IEEE Trans. on Neural Systems and Rehabilitation Engineering*, vol. 28, no. 5, pp. 1117–1127, 2020.
- [48] D. Freer and G.-Z. Yang, “Data augmentation for self-paced motor imagery classification with C-LSTM,” *Journal of Neural Engineering*, vol. 17, no. 1, p. 016041, 2020.
- [49] Z. Wang, S. Li, J. Luo, J. Liu, and D. Wu, “Channel reflection: Knowledge-driven data augmentation for EEG-Based BCIs,” *Neural Networks*, vol. 176, p. 106351, 2024.
- [50] M. Tangermann, K.-R. Müller, A. Aertsen, N. Birbaumer, C. Braun, C. Brunner, R. Leeb, C. Mehring, K. J. Müller, G. Mueller-Putz *et al.*, “Review of the BCI competition IV,” *Frontiers in Neuroscience*, vol. 6, p. 55, 2012.
- [51] W. Yi, S. Qiu, K. Wang, H. Qi, L. Zhang, P. Zhou, F. He, and D. Ming, “Evaluation of EEG oscillatory patterns and cognitive process during simple and compound limb motor imagery,” *PloS one*, vol. 9, no. 12, p. e114853, 2014.
- [52] D. Steyrl, R. Scherer, J. Faller, and G. R. Müller-Putz, “Random forests in non-invasive sensorimotor rhythm brain-computer interfaces: a practical and convenient non-linear classifier,” *Biomedical Engineering / Biomedizinische Technik*, vol. 61, no. 1, pp. 77–86, 2016.
- [53] B. Blankertz, R. Tomioka, S. Lemm, M. Kawanabe, and K.-r. Müller, “Optimizing spatial filters for robust EEG single-trial analysis,” *IEEE Signal Processing Magazine*, vol. 25, no. 1, pp. 41–56, 2008.
- [54] V. J. Lawhern, A. J. Solon, N. R. Waytowich, S. M. Gordon, C. P. Hung, and B. J. Lance, “EEGNet: A compact convolutional neural network for EEG-based brain-computer interfaces,” *Journal of Neural Engineering*, vol. 15, no. 5, p. 056013, 2018.
- [55] Y. Grandvalet and Y. Bengio, “Semi-supervised learning by entropy minimization,” in *Proc. Int’l Conf. on Neural Information Processing Systems*, Cambridge, MA, Dec. 2004, pp. 529–536.
- [56] K. Saito, D. Kim, S. Sclaroff, T. Darrell, and K. Saenko, “Semi-supervised domain adaptation via minimax entropy,” in *Proc. Int’l Conf. on Computer Vision (ICCV)*, Seoul, Korea, Oct. 2019, pp. 8049–8057.
- [57] Y. Jin, Z. Cao, X. Wang, J. Wang, and M. Long, “One fits many: Class confusion loss for versatile domain adaptation,” *IEEE Trans. on Pattern Analysis and Machine Intelligence*, vol. 46, no. 11, pp. 7251–7266, 2024.